The 9th European Congress on Computational Methods in Applied Sciences and Engineering
ECCOMAS Congress 2024
3–7 June 2024, Lisboa, Portugal

COMPARATIVE STUDY OF ORIFICE SHAPES ON SHOCK ABSORBER: IMPACT ON ENERGY DISSIPATION AND CAVITATION

Paulo A. S. F. Silva[1], Ahmed A Sheikh Al-Shabab[1] and Panagiotis Tsoutsanis[1], Martin Skote[1]

[1] School of Aerospace, Transport and Manufacturing, Cranfield University, Cranfield MK43 0AL, UK

Key words: Shock Absorber, CFD, Multiphase Flow, Cavitation, Orifice Design

Summary. Aircraft shock absorbers rely on orifice designs to control fluid flow and optimize damping performance. This study presents a computational fluid dynamics (CFD) analysis of circular, rectangular, semicircular, and cutback orifice profiles in oleo-pneumatic shock absorbers. Using OpenFOAM with the Schnerr-Sauer cavitation model and k-omega SST turbulence model, we investigated the effects of orifice shape and length-to-diameter (L/D) ratio on pressure drop, velocity distribution, cavitation inception, and discharge coefficients. Results show that rectangular orifices generate higher damping pressures but promote earlier cavitation, while semicircular shapes offer balanced performance with controlled cavitation. Circular designs demonstrate superior discharge coefficients across L/D ratios. This research provides insights for optimizing shock absorber performance, enhancing vehicle safety and passenger comfort.

1 Introduction

Shock absorbers are critical components in aircraft and automotive suspension systems, responsible for attenuating vibrations and dissipating kinetic energy during landing or over rough terrain. The damping performance and dynamic stability of these systems are dictated by complex fluid flows within hydraulic control elements, with orifices playing a pivotal role in creating pressure drops to develop controllable damping forces. However, excessive pressure reduction risks the onset of cavitation – the formation of vapor bubbles which can induce noise, component erosion, and performance loss if left uncontrolled. Previous studies have established correlations between orifice geometry and cavitation inception. Pearce and Lichtarowicz [1] and Nurick et al. [2] investigated the influence of geometry on discharge coefficients and cavitation characteristics in submerged orifices. Recent works by Ge et al. [3, 4, 5] have explored the effects of liquid properties, temperature, and cavitation number on cavitation dynamics in nozzles, while Apte et al. [6] and Li et al. [7] evaluated various turbulence models for simulating cavitating flows. In the context of shock absorbers, early research by Milwitzky and Cook [8] presented basic models for shock absorber dynamics during landing impact. More recent studies, such as those by Alonso et al. [9] and Ding et al. [10], have employed computational fluid dynamics (CFD) to analyze internal flows and calculate discharge coefficients in shock absorber orifices.

Despite these advancements, there remains a lack of comprehensive research exploring the impact of orifice shape and dimensions on the multiphase flow dynamics and damping performance of shock absorbers. This study aims to elucidate the complex interactions between orifice

geometry, cavitating flow dynamics, and damping performance of aircraft shock absorbers during drop-test conditions. The specific objectives are:

- To quantify the influence of orifice shape and length-to-diameter ratio on pressure drop, velocity distribution, and vapor formation using high-fidelity CFD analysis.
- To compare the discharge coefficients and damping loads of circular, rectangular, semi-circular, and cutback orifice profiles during critical conditions.
- To provide design guidelines for optimizing orifice geometry based on target shock absorber performance metrics.

2 Numerical Methods

This study employs the open-source CFD software OpenFOAM to investigate cavitating flow in shock absorber orifices. The compressible Unsteady Reynolds Averaged Navier-Stokes (URANS) equations are coupled with the volume of fluid (VOF) method for multiphase flow modeling. The governing equations for conservation of mixture mass, momentum, and energy are:

$$\frac{\partial \rho_m}{\partial t} + \nabla \cdot (\rho_m \mathbf{U_m}) = 0 \tag{1}$$

$$\frac{\partial (\rho_m \mathbf{U_m})}{\partial t} + \nabla \cdot (\rho \mathbf{U_m} \mathbf{U_m}) = -\nabla p_m + \nabla \cdot [\mu_m (\nabla \mathbf{U_m} + \nabla \mathbf{U_m}^T)] + \rho_m \mathbf{g} + \mathbf{F} \tag{2}$$

$$\frac{\partial (\rho E)}{\partial t} + \nabla \cdot [\mathbf{U_m}(\rho E + p)] = \nabla \cdot [k \nabla T] \tag{3}$$

where subscript m denotes mixture quantities, ρ is density, $\mathbf{U_m}$ is velocity, p is pressure, μ is dynamic viscosity, $\mathbf{g}$ is gravitational acceleration, $\mathbf{F}$ is surface tension force, E is total energy, k is thermal conductivity, and T is temperature.

The Schnerr-Sauer cavitation model is employed to capture phase change:

$$R = \frac{\rho_v \rho_l}{\rho_m} \alpha (1 - \alpha) \frac{3}{R_B} \sqrt{\frac{2|p - p_{sat}|}{3\rho_l}} \tag{4}$$

where R is the mass transfer rate, α is vapor volume fraction, R_B is bubble radius, and p_{sat} is saturation pressure.

Turbulence is modeled using the k-omega Shear Stress Transport (SST) model. The shock absorber geometry, illustrated in Figure 1, consists of upper and lower cylinders connected by a central orifice plate. Four orifice designs were tested: semicircle, cutback, rectangular, and circular, with length-to-diameter (L/D) ratios ranging from 0.5 to 1.28.

Table 1 summarizes the key simulation parameters. The piston motion is specified based on experimental stroke profiles for drop tests [8]. A polynomial equation of state is used for the oil, while nitrogen is treated as an ideal gas.

The grid independence was established through a refinement study and assessing the velocity magnitude at the orifice as can be seen in Figure 2, the final mesh containing 41.2k cells provide

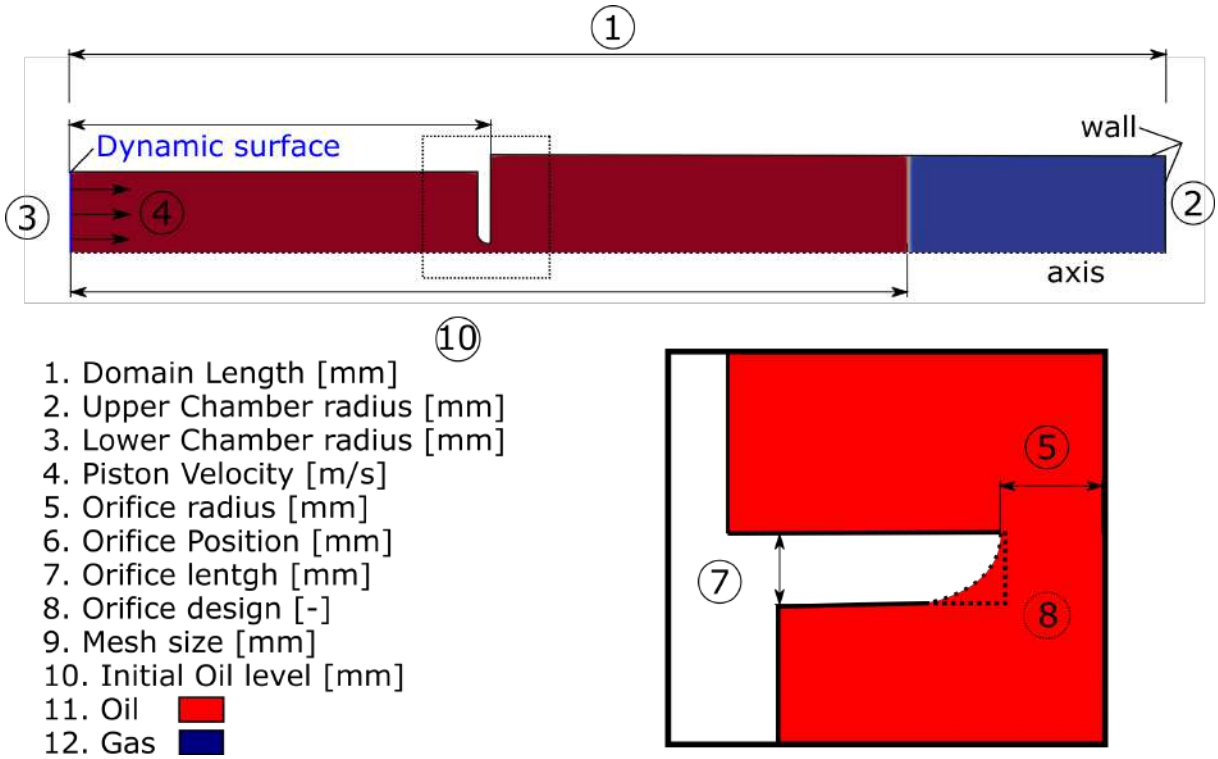

Figure 1: Geometry schematic of shock absorber

a balance between accuracy and computational efficiency. The PIMPLE algorithm is used for pressure-velocity coupling with a maximum Courant number of 10.

Table 1: Parameters for the shock absorber simulation

Parameter	Value
Domain length [mm]	505
Upper Chamber radius [mm]	45.27
Lower Chamber radius [mm]	37.31
Orifice radius [mm]	4.05
Orifice position [mm]	193.97
Orifice length [mm]	4.05-12.00
Oil level [mm]	386
Total simulation time [s]	0.15
Saturation pressure [Pa]	2300
Initial pressure [Pa]	299921.941
Initial fluid temperature [K]	300
Oil Density [kg/m^3]	867
Gas Density [kg/m^3]	1.205
Oil Kinematic Viscosity [m^2/s]	1.35×10^{-2}

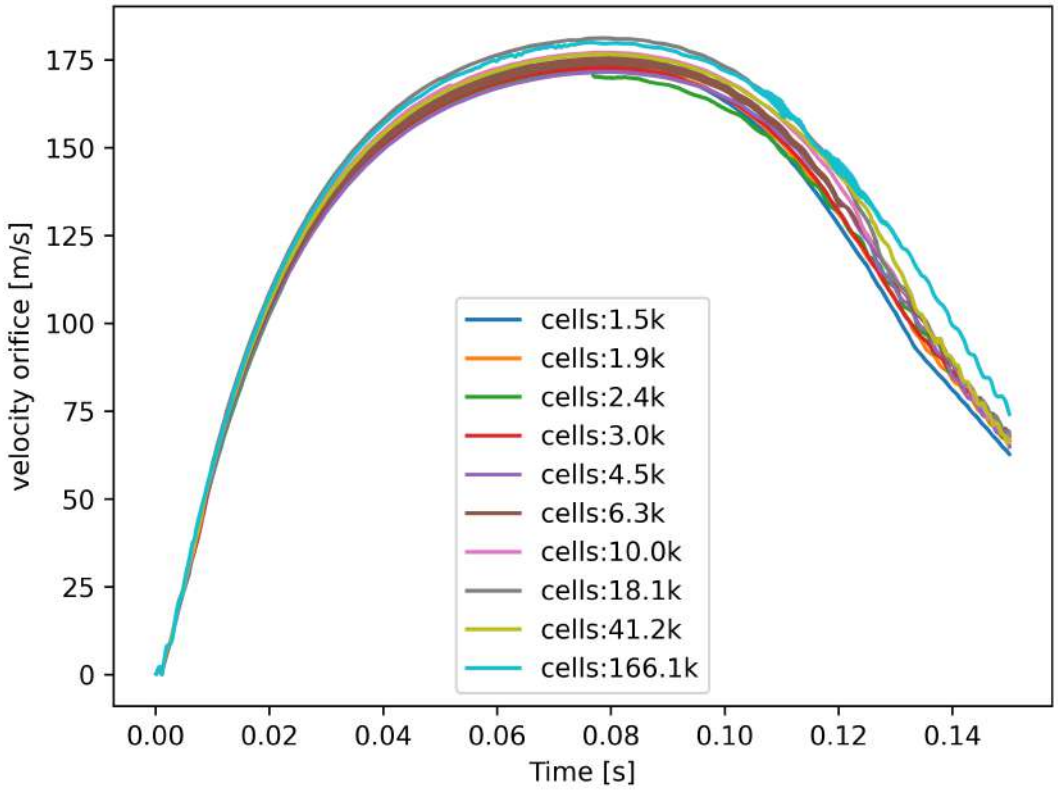

Figure 2: Grid independence study showing convergence of pressure (top) and velocitybottom at the orifice.

3 RESULTS AND DISCUSSION

Figure 3 illustrates the pressure drop across various orifice designs and L/D ratios as a function of stroke displacement. The rectangular orifice consistently produced the highest damping pressures, followed by the cutback, circular, and semi-circular designs. Increasing L/D ratio had a marginal effect on pressure drop for sharp-edged orifices (rectangular and cutback) but decreased it for circular shapes. The rectangular design exhibited the lowest average deviation (1.67%) across L/D ratios, indicating consistent performance.

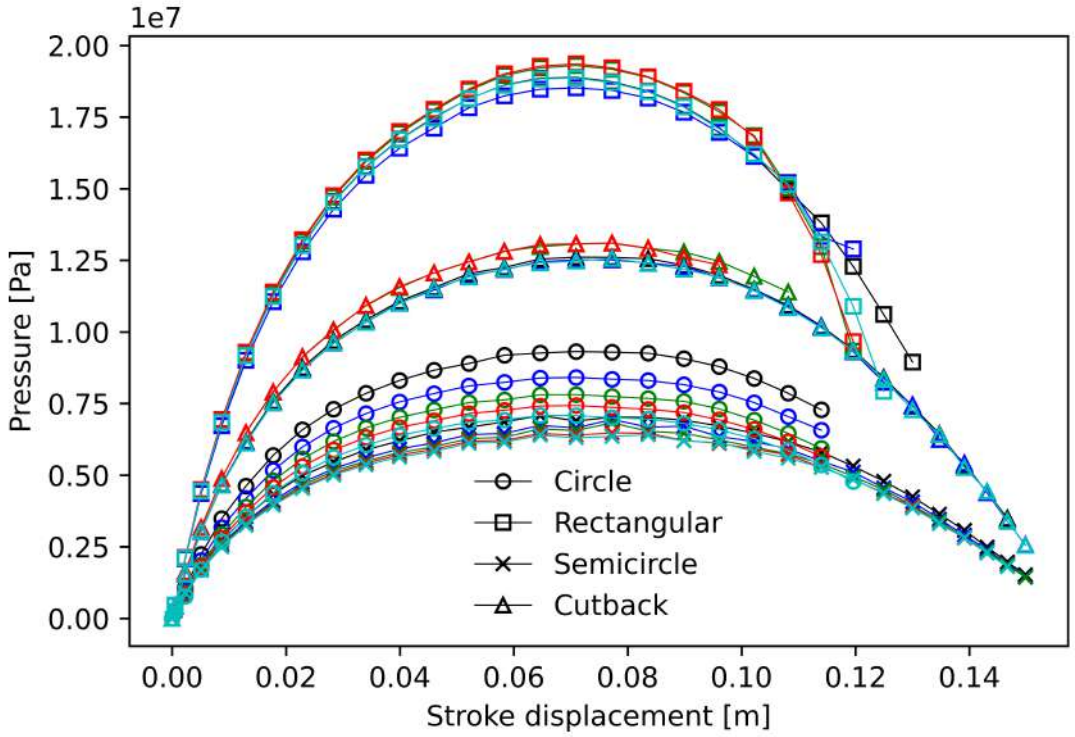

Figure 3: Pressure drop by stroke displacement for various orifice shapes and lengths according to line color Black ($L/D = 0.5$), Blue ($L/D = 0.69$), Green ($L/D = 0.89$), red ($L/D = 1.08$) and Cyan ($L/D = 1.28$)

Orifice velocity magnitudes varied significantly with shape profile, as shown in Figure 4. The rectangular geometry generated the highest velocities, often exceeding 125 m/s, with increasing L/D ratio promoting higher velocities. Cutback shapes experienced the lowest peak velocities due to greater flow separation. Circular designs showed minimal variation (0.41% for circle, 0.18% for semicircle) across L/D ratios, demonstrating robust velocity profiles.

Figure 5 depicts the change in averaged density at the orifice, indicating cavitation onset.Sharp density drops for rectangular, circular, and cutback shapes indicate vapor formation at the orifice. The semi-circular shape maintained constant density, suggesting downstream

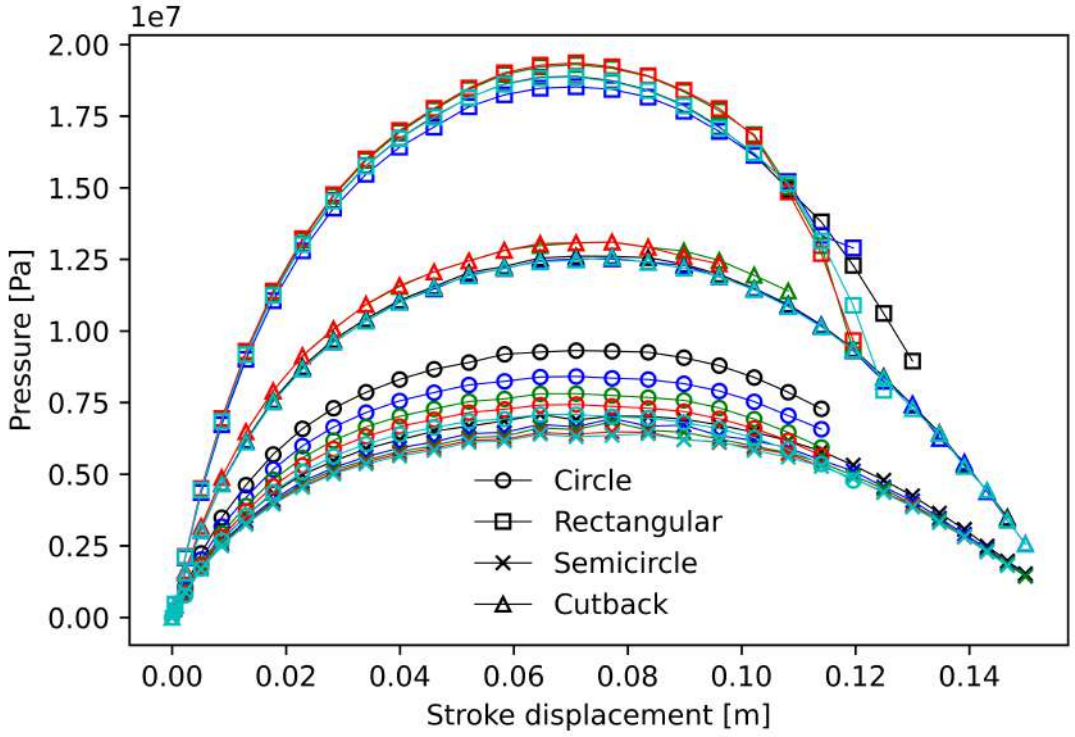

Figure 4: Orifice Velocity by stroke displacement for various orifice shapes and lengths according to color: Black ($L/D = 0.5$), Blue ($L/D = 0.69$), Green ($L/D = 0.89$), red ($L/D = 1.08$) and Cyan ($L/D = 1.28$)

cavitation development. Increasing orifice length had limited influence on cavitation behavior at the orifice.

Figure 6 presents a comparative study of oil-gas interaction for various orifice shapes at two critical time instances. At t=0.025s, the rectangular profile showed strong disturbances from vapor structures, while the circular shape exhibited minimal upstream cavitation influence. At t=0.05s, recirculation patterns became apparent, re-energizing the shear layer and highlighting the complex flow dynamics.

3.1 Discharge Coefficient Comparison

Table 2 compares the averaged discharge coefficients (Cd) across orifice shapes and L/D ratios with theoretical predictions. Circular and semi-circular designs showed superior performance with Cd values consistently between 0.94-0.96, significantly higher than theoretical predictions. The rectangular orifice exhibited the lowest Cd values (0.62-0.66), closer to theoretical predictions, possibly due to flow instabilities and sensitivity to entry geometry.

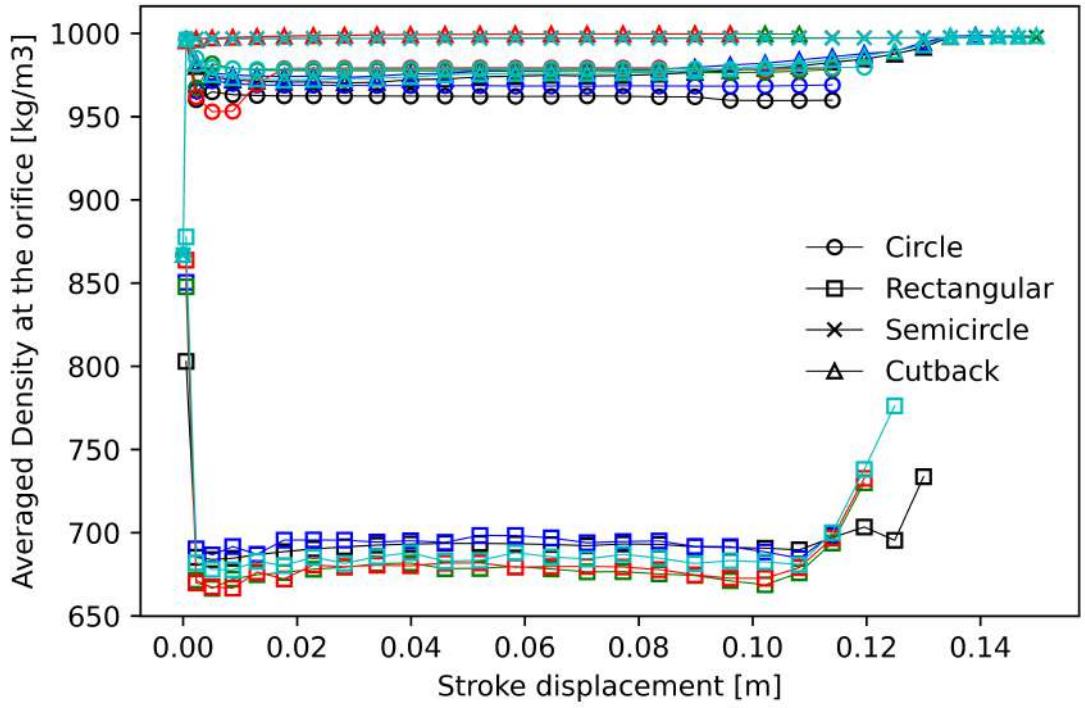

Figure 5: Density at the orifice probe by stroke displacement for various orifice shapes and lengths according to color: Black $L/D = 0.5$, Blue $L/D = 0.69$, Green $L/D = 0.89$, red $L/D = 1.08$ and Cyan $L/D = 1.28$

Table 2: Time-averaged discharge coefficients for various orifice shapes across L/D ratios

L/D	Rectangular	Circle	Semi Circle	Cutback	Theory [11]
0.5	0.66	0.94	0.95	0.85	0.65
0.69	0.64	0.95	0.94	0.94	0.68
0.89	0.62	0.95	0.95	0.98	0.71
1.08	0.62	0.95	0.96	0.93	0.77
1.28	0.62	0.95	0.96	0.94	0.78

4 Conclusions

This study presents a comprehensive CFD analysis of the influence of orifice design on the internal cavitating flow and energy dissipation in oleo-pneumatic shock absorbers. Key findings include:

- The rectangular orifice design exhibited the highest damping pressure drop and the steepest

pressure gradient along the orifice length, making it favorable for energy dissipation.

- The cutback and rectangular geometries demonstrated early cavitation inception, while the circular shapes resisted initial vapor formation, highlighting the strong influence of orifice entrance sharpness on cavitation characteristics.
- The semi-circular profile achieved a balance between smooth flow and controlled cavitation, optimizing the operating range.
- When examining the impact of L/D variation on results, we observed a moderate level of difference across all designs investigated. Notably, the pressure drop across the rectangular orifice exhibited the most significant variation, reaching up to 10%.
- The discharge coefficient was significantly affected by orifice shape and L/D ratio, with the circular and semi-circular designs showing superior performance compared to the rectangular design.

REFERENCES

[1] Pearce, I. D., and A. Lichtarowicz. "Discharge performance of long orifices with cavitating flow." Proceedings of Second Fluid Power Symposium, Guildford, UK. 1971.

[2] Nurick, W. H. "Orifice cavitation and its effect on spray mixing." (1976): 681-687.

[3] Ge, Mingming, et al. "Cavitation dynamics and thermodynamic effects at elevated temperatures in a small Venturi channel." International Journal of Heat and Mass Transfer 170 (2021): 120970.

[4] Ge, Mingming, et al. "Intensity and regimes changing of hydrodynamic cavitation considering temperature effects." Journal of Cleaner Production 338 (2022): 130470.

[5] Ge, Mingming, et al. "Dynamic mode decomposition to classify cavitating flow regimes induced by thermodynamic effects." Energy 254 (2022): 124426.

[6] Apte, Dhruv, Mingming Ge, and Olivier Coutier-Delgosha. "Numerical investigation of a cavitating nozzle for jetting and rock erosion based on different turbulence models." Geoenergy Science and Engineering 231 (2023): 212300.

[7] Li, L., Xu, Y., Ge, M., Wang, Z., Li, S., & Zhang, J. (2023). "Numerical investigation of cavitating jet flow field with different turbulence models". Mathematics, 11(18), 3977.

[8] Milwitzky, Benjamin, and Francis E. Cook. Analysis of landing-gear behavior. No. NACA-TN-2755. 1952.

[9] Alonso, M., and Á. Comas. "Modelling a twin tube cavitating shock absorber." Proceedings of the Institution of Mechanical Engineers, Part D: Journal of Automobile Engineering 220.8 (2006): 1031-1040.

[10] Ding, Y. W., Wei, X. H., Nie, H., & Li, Y. P. (2018). "Discharge coefficient calculation method of landing gear shock absorber and its influence on drop dynamics." Journal of vibroengineering, 20(7), 2550-2562.

[11] Dixon, John C. The shock absorber handbook. John Wiley & Sons, 2007.

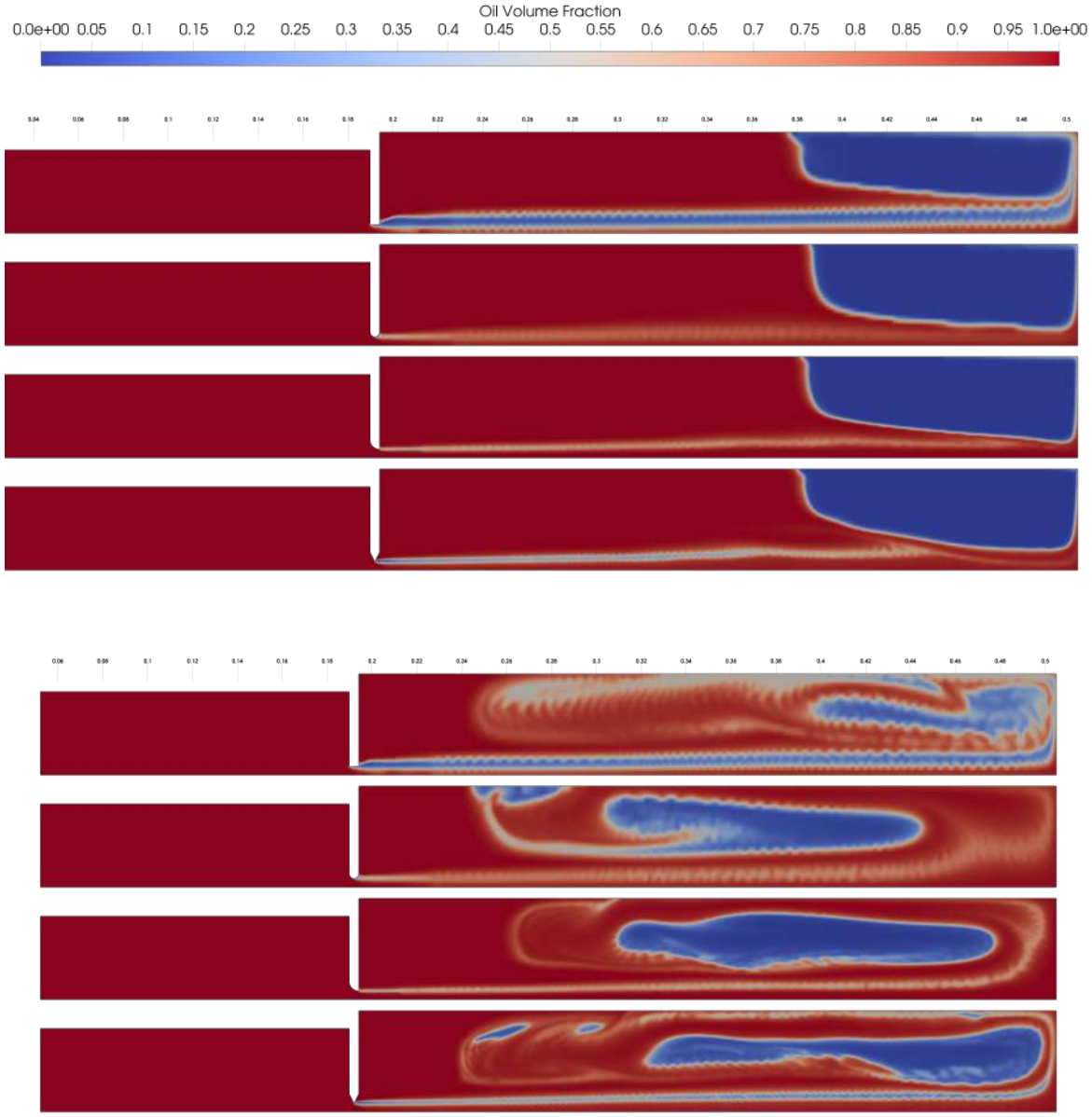

Figure 6: Volume fraction of liquid for all designs for L/D=0.5 at t=0.025s and t=0.05s